Journal of Polymer Science

WILEY

JOURNAL OF POLYMER SCIENCE

PERSPECTIVE OPEN ACCESS

Synergies in Self-Assembly—From Supramolecular Polymers to Defined Hierarchical Superstructures

Klaus Kreger[1,2] | Florian Behrendt[1,2] | Johannes C. Brendel[1,2]

[1]Macromolecular Chemistry I, University of Bayreuth, Bayreuth, Germany | [2]Institute of Macromolecular Research (BIMF) and Bavarian Polymer Institute (BPI), University of Bayreuth, Bayreuth, Germany

Correspondence: Johannes C. Brendel (johannes.brendel@uni-bayreuth.de)

Received: 2 April 2025 | **Revised:** 4 June 2025 | **Accepted:** 5 June 2025

Funding: This work was supported by Deutsche Forschungsgemeinschaft (517761335).

Keywords: amphiphilic self-assembly | hierarchical materials | nano-/mesostructures | non-covalent interactions | supramolecular chirality

ABSTRACT

Nature creates hierarchical, self-assembling structures across all length scales to achieve superior properties, for example, in mechanics, photonics, reactivity and adaptability. These hierarchical structures are well defined in both form and function, although generally only a limited number of building blocks are used. In natural systems, chirality, precise sequencing of macromolecules, and combinations of non-covalent interactions are known to play a central role in the formation of hierarchical structures and superstructures, suggesting that synergies between different structure-defining elements are crucial. In this perspective, we highlight selected examples from nature and present artificial examples exemplifying a transition from supramolecular polymers to structures with higher levels of aggregation. These include supramolecular systems based on chiral building blocks, which typically allow for hierarchical structures with tailored shapes and tuned helicity but also defined lateral dimensions. We also outline artificial supramolecular systems combining orthogonal secondary interactions, which allow the hierarchical structure to be confined to defined dimensions and shapes. Finally, we briefly discuss selected applications related to the hierarchy in the bulk or the corresponding surface of hierarchically structured systems. We also propose guidelines for defined hierarchical structures with potential to enhance light harvesting or to create artificial supramolecular antibodies.

1 | Introduction

Self-assembly is a key concept in nature to create objects from the nanoscopic to the macroscopic scale, providing outstanding and unsurpassed characteristics in form, shape, and function [1]. In living matter, self-assembly processes are more often energy dependent than in equilibrium, leading to features such as intrinsic self-healing and adaptivity, which also enable the reconfiguration of mechanical properties on demand, including strength and toughness, as well as elasticity and flexibility of the entire self-assembled structure [1–4]. One intriguing aspect is that nature uses only a limited number of building blocks to realize a large variety of different structural components [1]. A prominent example is collagen, which constitutes more than 30% of the proteome, that is, the total protein content, in human bodies [3]. Collagen is an integral part of a range of structural components with mechanical properties precisely tailored to their intended use, such as skin, tendons, and bone. This is achieved by forming superstructures at multiple hierarchical levels, with the primary structure being based on polypeptides composed of hundreds of amino acids. Three of these structural polypeptides subsequently assemble into a secondary structure via triple helix formation into the collagen molecule, with a length of about 300 nm and a diameter of about 1.5 nm (Figure 1a). These collagen molecules further aggregate laterally and longitudinally into fibrils with diameters of about 30 nm. In the case of bones, nanoplatelets of hydroxyapatite crystals are incorporated into the collagen fibrils, creating a nanocomposite

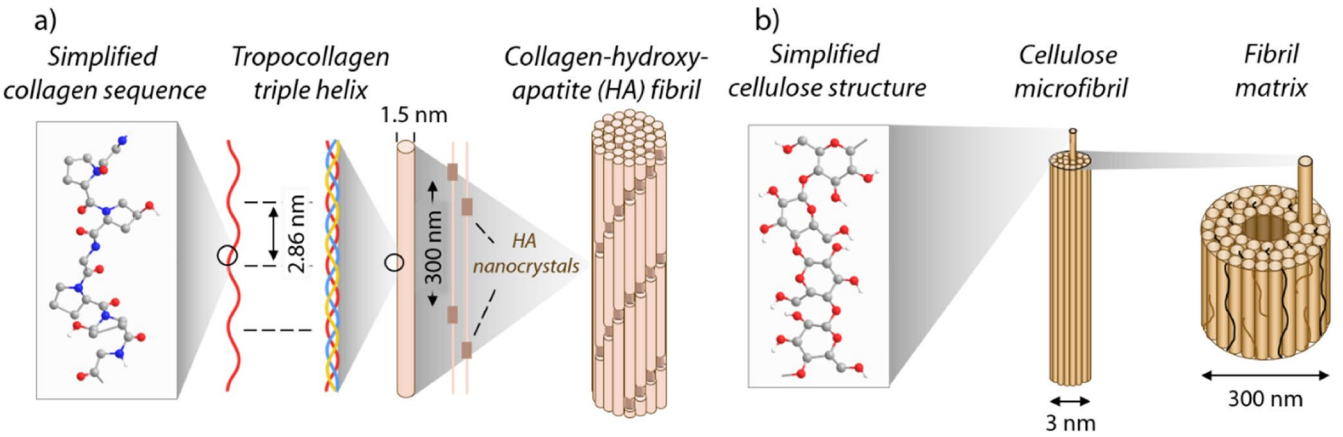

FIGURE 1 | Hierarchical superstructures in nature. (a) Structural components built from polypeptides including assembly into collagen molecules via triple helix formation in a first step and subsequent aggregation to collagen fibrils. In bones, nanoplatelets of hydroxyapatite (HA) are embedded in a defined manner. (b) The main structural components in plants are cellulose-based structures, which initially form microfibrils and are subsequently arranged in a defined fibril matrix.

with high stiffness. On a further level, several of these fibrils, together with proteoglycans, highly glycosylated proteins, form fibers featuring mm lengths and diameters in the μm range. This and higher hierarchical levels allow bridging the gap to the macroscopic scale, but also tuning the mechanical properties using hard and soft components, as well as different levels of porosities [4, 5]. These complex organized superstructures provide mechanisms for mechanical deformations and thus enable nature to cover Young's moduli in the MPa to the GPa range.

In plants, the structural components are predominantly based on cellulose rather than proteins. Similarly, the mechanical properties, among other things, are tuned by establishing different hierarchical levels. This includes, for instance, in bamboo and palm stems the formation of superstructures such as microfibrils with diameters of 3 nm and their subsequent organization into the fibril matrix with diameters of about 300 nm, which can be regarded as oriented cellulose in a hemicellulose/lignin matrix (Figure 1b) [1]. On further levels, this kind of structural nanocomposites comprise elongated pores, which leads, for example, to the extraordinary mechanical features of bamboo [5, 6].

Considering the underlying species, nature uses macromolecular building blocks. Those consist of monomers, for example, amino acids or nucleic bases, which are precisely covalently connected in sequence and length as found in polypeptides and DNA. These polymers represent the primary structure. The first level of intra- or intermolecular aggregation via non-covalent interactions leads to secondary structures such as mono, double, and triple-type helical fibers (Figure 2a) [7]. While mimicking natural polymers in their precision remains challenging to achieve, a plethora of synthetic building blocks have been developed, which adapt a similar helical structural organization into secondary structures via non-covalent interactions such as ion-dipole and dipole–dipole interactions, hydrogen bonding, π-π stacking, and weak Van der Waals interactions (Figure 2b) [8]. Prominent examples include 1,3,5-benzenetricarboxamides (BTA), which form three strands of hydrogen bonds helically arranged along the columnar axis, and perylene bisimides (PBI), which predominantly stack via π-π interactions, here supported by hydrogen bonds into a helical arrangement. Similar helical arrangements can be found for aromatic amide foldamers or oligo-squaraines. These self-assembled secondary structures are often referred to as supramolecular polymers. Thus, supramolecular polymers can be regarded as linear chains of (macro)molecular building blocks connected via highly directional and non-covalent interactions [9, 10]. The term supramolecular polymer is not necessarily limited to linear polymer-type structures. Supramolecular polymerization can also proceed in a sheet-like, 2-dimensional manner or lead to other complex structures [11, 12].

Non-covalent interactions that establish during the self-assembly process of supramolecular polymers are intrinsically more reversible than covalent bonds. Thus, the formation and dimensional stability of a self-assembled structure strongly depend on the given set of conditions, including the solvent, the temperature, and the concentration, besides the molecular structure of the building blocks. Variations of these parameters may favor self-assembly or disassembly but also influence the dynamic nature of the assembly, i.e., the ability to exchange individual building blocks. Contrary to living matter, artificial self-assembled systems or supramolecular polymers are more likely to be in equilibrium and lack adaptivity [13]. In particular, when in a dynamic state, assemblies tend toward the global minimum of the energy landscape and thus adapt a stable configuration. However, self-assembled systems may also end up in a local minimum with energy barriers preventing a dynamic exchange and become kinetically trapped during the assembly process. In this case, the thermodynamic equilibrium may not be reached, and the assembly pathway has a strong impact on the final structure of the supramolecular polymer [14].

Taking these considerations a step further, the set of conditions decides on the structural outcome beyond the formation of supramolecular polymers, namely the formation of objects with a higher level of aggregation. The latter can be considered as the tertiary or quaternary structure and thus as (hierarchical) superstructures. A widely investigated and prototypical synthetic supramolecular motif is the above-mentioned BTA, where these considerations can nicely be

exemplified given numerous derivatives being investigated by multiple research groups [15]. The arrangement in the columnar stacking driven by three strands of hydrogen bonds was demonstrated by Lightfoot et al. on crystals of *N,N′,N″*-tris(2-methoxyethyl)-1,3,5-benzenetricarboxamide processed from ethanol [16]. Meijer et al. visualized the formation of supramolecular polymers with a diameter of about 5 nm close to the molecular diameter and extensive lengths in the μm-range from aqueous solutions using a BTA with three large hydrophobic/hydrophilic side groups in the periphery (Figure 3a) [17, 19]. Recently, cryogenic transmission electron microscopy and cryo-electron tomography were used to show that this particular BTA forms double helices [20]. This demonstrates that state-of-the-art electron microscopy techniques are useful for visualizing the structure of supramolecular polymers at the nanoscale [21]. Equally important, subtle variations in the molecular structure have a strong influence on the resulting morphology. Thus, supramolecular polymer formation to fiber-like structures as well as the observed dynamic exchange require a delicate balance between the lengths of the hydrophobic/hydrophilic side groups [22, 23]. The centrosymmetric arrangement of such large side groups on all amide units prevents further excessive aggregation in solutions. BTAs with much shorter nonpolar side groups often feature a significant tendency to form larger bundles composed of supramolecular columns, which can be regarded as a tertiary

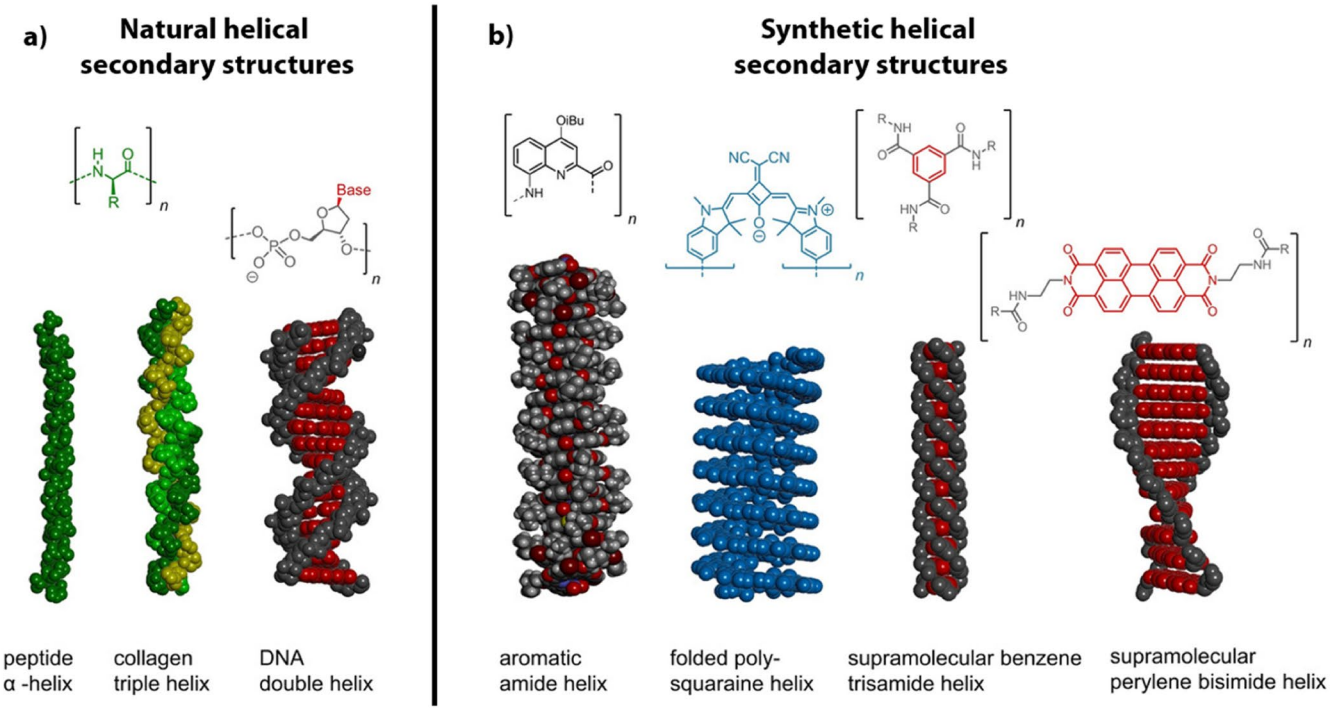

FIGURE 2 | Examples of natural macromolecular building blocks such as polypeptides, collagen and DNA (a), together with synthetic building blocks such as aromatic amide foldamers, oligo-squaraines, 1,3,5-benzenetricarboxamides and perylene bisimides (b), capable of forming helical secondary structures. Adapted with permission [7]. Copyright © 2020 Wiley-VCH Verlag GmbH & Co. KGaA.

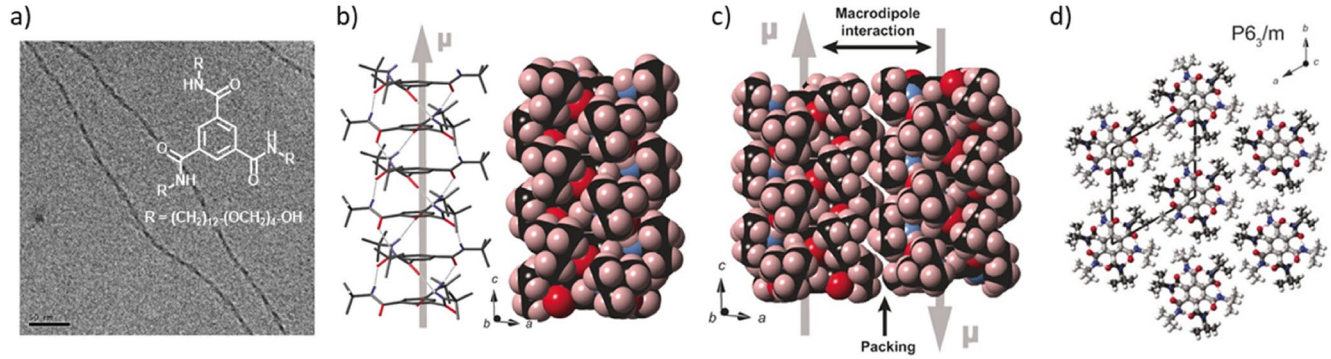

FIGURE 3 | (a) Cryo-TEM image of a supramolecular polymer of a BTA with long hydrophobic/hydrophilic side groups (scale bare represents 50 nm). Adapted under the terms of the CC-BY 3.0 license with permission [17]. Copyright © 2013, The Authors, published by the Royal Society of Chemistry. (b) A columnar stack of *N,N′,N″*-tris(1,1-dimethylethyl)-1,3,5-benzenetricarboxamide features a macrodipole across the columnar axis [18]. (c) The macrodipole interaction compensates via antiparallel alignment [18]. (d) Further bundling leads to a hexagonal arrangement (P6$_3$/m) of the supramolecular columns [18]. Adapted under the terms of the CC-BY license with permission [18]. Copyright © 2017 The Authors, published by Wiley-VCH Verlag GmbH & Co. KGaA.

structure. One driving force for further aggregation is related to the three helical strands of hydrogen bonds that point in the same direction. As a result, they form a pronounced macrodipole along the columnar axis (Figure 3b). In general, dipole–dipole interactions scale with r^{-3}, and consequently, the interaction between the macrodipoles is more present in BTAs with short side groups [24]. The macrodipoles subsequently compensate themselves by arranging the supramolecular columns in an antiparallel manner (Figure 3c). In this situation, the side groups can also be very densely packed, which for BTAs ultimately leads to larger bundles in a (pseudo)hexagonal arrangement (Figure 3d) [18].

To put this into context: A BTA with tert-butyl side groups as shown in Figure 3b exhibits a molecular diameter of about 1.5 nm. Upon self-assembly into a bundle of nanofibers with 100 nm in diameter, this represents about 3500 densely packed supramolecular columns in the bundle cross-section. The given examples demonstrate that there can be a pronounced variation between the dimensions of single supramolecular polymers and bundles of supramolecular polymers depending on the structural design of the building block, but also other parameters may play a significant role. Such bundles of supramolecular columns already bear resemblance to the hierarchical structure formation found in nature, but often exhibit a significant distribution of the bundle diameter and thus of the number of supramolecular polymers involved in bundle formation. Perfect control over the lateral dimensions and the hierarchical order of the superstructure is therefore not easily accomplished, and the complexity of nature's order remains yet out of reach.

But how can we shape supramolecular polymers into defined hierarchical superstructures in a more controlled manner? In this perspective, we like to highlight two considerations, which have already proven to control the shape as well as the lateral dimensions beyond single supramolecular polymers on the nano- and mesoscale. For instance, one consideration is related to delicate conformational restrictions which are encoded in the building block. In particular, chirality can drive the structure formation in a predetermined way by creating a distinct helicity, which may also lead to a lateral confinement. Also, the introduction of a second orthogonal driving force that does not interfere with the central supramolecular motif may facilitate the confinement of the superstructure growth. In the following sections, we provide only a small number of selected examples, which illustrate each concept. For a more comprehensive overview, we refer to excellent reviews in each of the chapters.

2 | Synergies in Supramolecular Architectures to Superstructures—Chirality

A general aspect that seems to be beneficial for the realization of defined superstructures is the use of chiral molecules similar to nature. Chirality is a ubiquitous phenomenon that spans all length scales, from the subatomic to the galactic scale. In living matter, chirality plays an exposed and decisive role, which means that function is due to the superstructure form. As shown in Figure 2 (left) for natural polymers, the primary structure leads to the secondary structures via inter- and intramolecular interactions and upon further aggregation to structures with higher hierarchical levels. In this way, nature establishes defined structures mainly via non-covalent interactions, which are critical for the function, for example for recognition and reaction purposes. Thus, it is not unexpected that there are numerous artificial molecular building blocks that contain chiral side groups [25]. Introducing such groups into molecular building blocks can lead to self-assembled structures with supramolecular chirality, which in simple terms means that the self-assembled structures themselves exhibit helicity or other complex structures with chirality [25, 26]. Chiral side groups are also often introduced into the building blocks for analytical purposes to monitor the self-assembly process via circular dichroism (CD) spectroscopy [27]. In the simplest case, when two light-absorbing chromophores approach each other and aggregate, this leads to an interaction of the transition dipole moments and thus to exciton coupling. In the case of chiral molecules, the aggregates are twisted to each other, leading to a bisignate signal in the CD spectrum, also referred to as the Cotton effect. In supramolecular aggregates using building blocks with the same enantiopure isomers, that is, the R- or S- isomers, the predominant formation of left- or right-handed helices is assigned in this way, which are referred to as M- (minus) or P- (plus) helices [28]. In the case of BTAs with chiral side groups in the periphery, this is attributed to the preferentially clockwise or counterclockwise orientation of the hydrogen bond triple helix or ultimately the twist of the central benzene ring [29]. In systems with two enantiopure compounds at the same ratio, two sorts of supramolecular polymers with the opposite helicity may evolve in a self-sorting manner but possibly with different energy. If one of the enantiomers is in excess, the excess building block may ultimately dictate the resulting helicity, which is known as the majority rules effect [30, 31]. Upon mixing small amounts of chiral building blocks with non-chiral building blocks, the supramolecular aggregates may adapt predominately the chiral supramolecular polymer structure, which is known as the sergeant and soldier principle [31, 32]. This leads to a chiral amplification, and it suggests that chiral supramolecular polymer formation is driven by conformational arrangements due to the chiral side groups, which eventually leads to a structure with lower energy [26]. The use of different molecular building blocks requires a dynamic exchange between the monomeric species and the self-assembled structures. Therefore, CD spectroscopy is often performed in suitable organic solvents. In aqueous media, the self-assembled structures have lower dynamics and more pronounced stability, so that more time is required for the chiral amplification to come into full effect. In addition, building blocks with solubilizing groups such as ethylene glycols can lead to turbid solutions in temperature-dependent measurements, as the lower critical solution temperature is exceeded, making it difficult to adequately study chiral amplification [33].

A positive or negative Cotton effect is also observed when non-chiral building blocks are used in the presence of enantiopure (R- or S-) solvents, suggesting that the preferential formation of a supramolecular polymer with pronounced helicity is driven by the chiral solvent [34]. A similar behavior can be observed in the presence of appropriate surfactants [35]. In this context, other more trivial external triggers for the formation of supramolecular polymers with preferential helicity are also known, such as stirring in a specific direction [36].

The visualization of such small structures with helicity and dimensions close to the molecular diameter, however, still remains a challenge [20].

At higher hierarchical levels, chiral molecular building blocks lead to chiral hierarchical or complex self-assembled structures with appealing shapes and morphologies in a similar manner, although it remains important to mention that a clear understanding and correlation between the molecular chirality and the structural helicity across the different length scales is not fully established [26]. As described above, building blocks with enantiopure isomers lead to supramolecular polymers with M- or P-helices and subsequent hierarchical structures with clockwise or counterclockwise spiral shapes. Depending on the central supramolecular motif leading to the basic structure (1D fiber, 2D ribbons, etc.) and the potential difference in conformational arrangements, this results in the realization of various known hierarchical structures with higher complexity if chiral side groups are employed. Figure 4 schematically shows some selected helical assemblies with higher hierarchical levels. A very large number of small molecular or polymeric building blocks are known for the realization of such or similar helical architectures. Therefore, we refer to several excellent and comprehensive reviews on supramolecular assemblies using chiral (macro)molecules for further reading [25, 26, 37].

In brief, helical architectures may be based on 1D or fiber-based structures, which can further assemble into single-helical fibers with spiral morphology or also homo-chiral assemblies, double-helical fibers containing two intertwined fibers, as well as bundles of helical fibers comprising two or multiple fibers. Similarly, 2D hierarchical structures are known to self-assemble into ribbon-like structures. These ribbon-like structures can further form twisted ribbons, helical ribbons, and chiral tubules [25, 26, 38]. In all these different kinds of hierarchical structures, the chiral side groups guide the structure formation along the different length scales.

Apart from the sense of chirality, another interesting aspect is that distinct chiral molecular building blocks allow for the formation

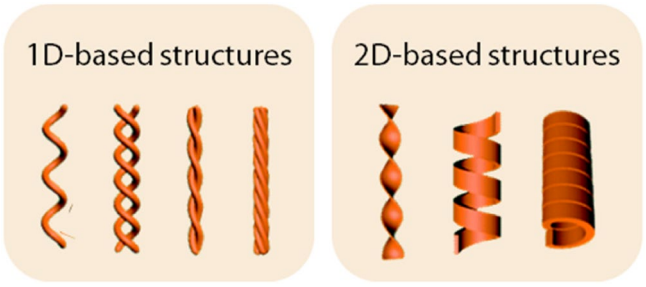

FIGURE 4 | Selected examples of schematic hierarchical or complex structures self-assembled from molecular building blocks with chiral side groups: 1D-based hierarchical structures may include single-helical fibers, double-helical fibers and helical bundles consisting of two or multiple fibers. 2D-based hierarchical structures may include twisted ribbons, helical ribbons, and chiral tubules. Adapted under the terms of the CC-BY 3.0 license with permission from the Royal Society of Chemistry [26]. Copyright © 2022, The Authors, published by The Royal Society of Chemistry.

of spiral or twisted structures with comparable high uniform lateral dimensions that are clearly larger than the molecular diameter of the building block. Early examples were already documented in the last century. For instance, Terech et al. studied in the mid-80s and later the self-assembly of various steroids such as a nitroxide-substituted steroid derivative in cyclohexane (Figure 5a) [39, 42, 43]. By investigating dried samples, they found fibrous helical structures with rather uniform average diameters of 26 nm, which comprise a pitch of about 50 nm [39]. These chiral helical fibers are partially connected and intertwined with each other in a defined manner. Loosely connected fibers can fold back and create a further hierarchical level. Another early example is based on the organogelator, 1,3:2,4-bis(dibenzylidene)sorbitol, which was investigated by the research group of Wittmann et al. In a similar manner, they found rather uniform helical superstructures that are intertwined creating larger structures with higher hierarchical levels [44]. Similar observations were found, namely uniform helical superstructures, when other derivatives such as 1,3:2,4-di(3,4-dichlorobenzylidene) sorbitol were self-assembled from non-polar solvents [45]. Unlike building blocks with chiral moieties, which are a central part of the core, George et al. and Ajayaghosh et al. studied the self-assembly of elongated conjugated chromophores based on oligo(p-phenylenevinylene) with two chiral side groups based on (S)-3,7-dimethyloctanol, which are attached to the middle benzene group (Figure 5b) [40, 46]. During self-assembly in non-polar solvents, left-handed helical assemblies were found. Interestingly, upon increasing the concentrations, these helical ribbon assemblies seem to intertwine to form a further hierarchical level of helical structures with a pitch of about 150 nm.

An example of chiral superstructure formation based on a discotic core with chiral side groups was reported by Bose et al. They synthesized BTAs containing various amino acid methyl esters as side groups, including a BTA with three peripheral L-valine methyl esters (Figure 5c) [41]. When self-assembled from a methanol–water mixture, the crystal structure elucidation shows a hexagonal unit cell with the space group $P6_3$. As previously shown by Lightfoot et al., the BTA, driven by three strands of hydrogen bonds, stacks in a columnar arrangement representing the secondary structure. X-ray analysis also indicates that there is an additional interaction between the peripheral ester groups. Upon self-assembly and sonication, a tertiary structure of about 40 nm in diameter is found. These bundles of columnar stacks feature a spiral morphology. Upon further aggregation, three of these tertiary structures are intertwined in a triple helical fashion leading to a defined nanofiber with a diameter of about 140 nm. Similar hierarchically twisted superstructures are also observed for C3-symmetric trisamides with larger conjugated cores, based on a central benzene unit substituted by three diacetylene moieties in the 1,3,5 position [47]. Although the prototypical C3-symmetric molecular design is highly beneficial to realize fiber-like structures, it is not necessarily required to prepare hierarchically twisted fiber-like structures.

All in all, chiral side groups in molecular building blocks leading to supramolecular polymers and consequently to hierarchical structures have proven to be a powerful tool to produce superstructures with pronounced supramolecular chirality. Although additional strong non-covalent interactions are not necessarily required, the morphology of the superstructure can be guided by chirality, which is most likely driven by conformational

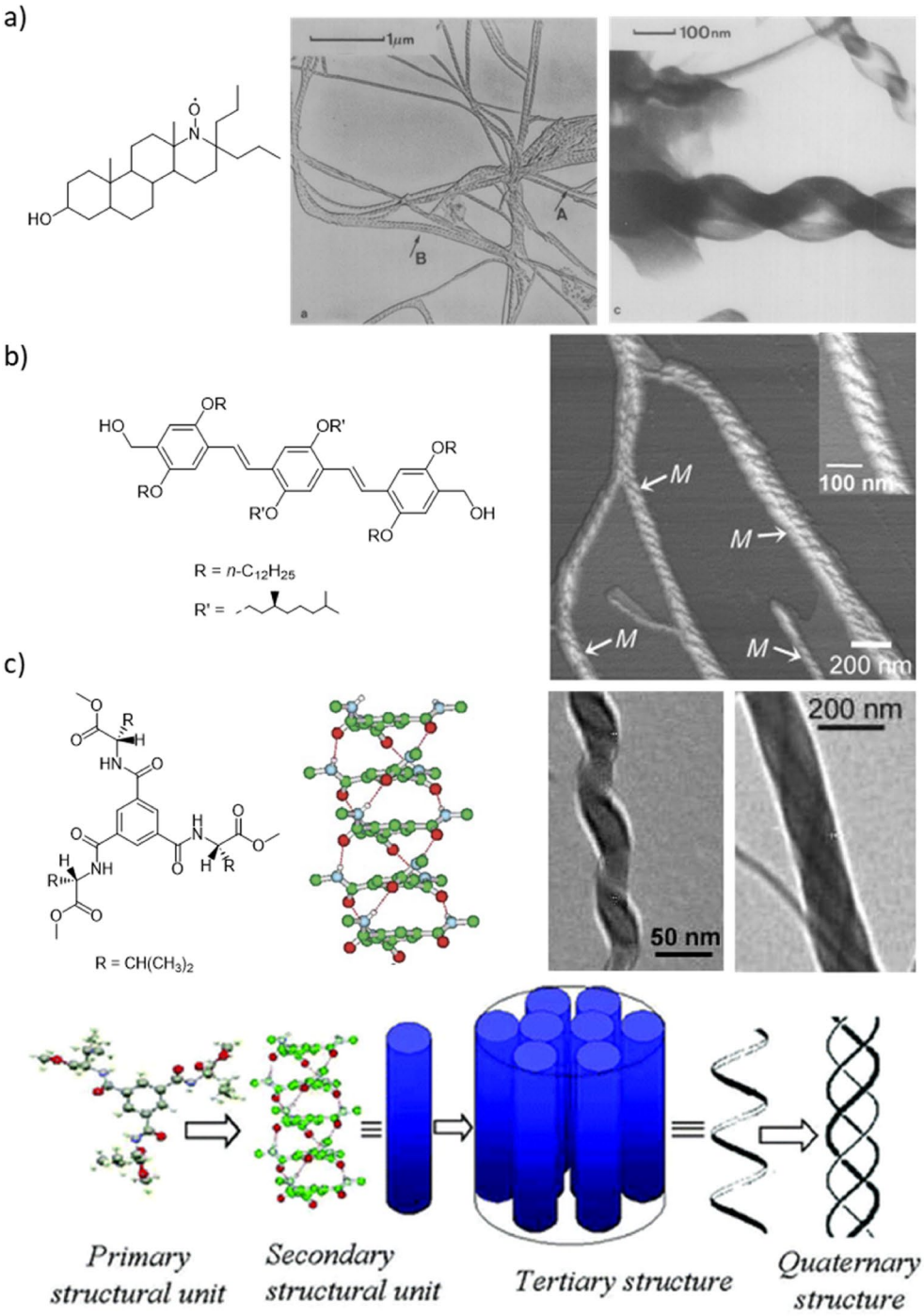

FIGURE 5 | Defined helical superstructures based on various chiral building blocks. (a) Steroid derivatives processed from cyclohexane and dried lead to long, partially interconnected fibrous helical structures with rather uniform diameters of about 26 nm. Shorter helical structures may fold back to form intertwined structures. Adapted with permission [39]. Copyright © 1988 Elsevier. (b) Oligo(p-phenylenevinylenes) with two chiral side groups lead to left-handed helical assemblies when processed from non-polar solvents. AFM images reveal helical ribbon assemblies, which intertwine to form further hierarchical helical assemblies. Adapted with permission [40]. Copyright © 2006 Wiley-VCH Verlag GmbH & Co. KGaA. (c) Helical superstructures based on a BTA with chiral L-valine methyl ester side groups. They assemble into columnar stacks with triple helical arrangement of the hydrogen bonds, which further forms a helical spiral structure with a diameter of about 40 nm. Three of these helical aggregates further assemble yielding nanofibers with diameters of about 140 nm. The lower row shows a schematic representation starting from primary to secondary to tertiary and quaternary structures. Adapted with permission [41]. Copyright © 2006 Royal Society of Chemistry (c).

arrangement and energy minimization, leading to a synergistic effect between the central supramolecular motif and the chiral side groups. In distinct cases, the structure becomes confined to a present lateral dimension, but it remains hardly possible to relate these dimensions to or even dictate it by the molecular design of the chiral building block.

3 | Synergies in Supramolecular Architectures to Superstructures—Orthogonal Secondary Interactions

Apart from the chirality aspect, the introduction of a second driving force or supramolecular interaction represents another possibility to achieve a structural confinement of supramolecular assemblies. The decisive factor is that it is not interfering with the central supramolecular motif. One option is the combination of supramolecular stacking by hydrogen bonding with a secondary interaction. 2-Ureido-4-pyrimidinones (UPy), for example, form dimers by complementary hydrogen bonding, which can then stack into columnar assemblies via additional lateral hydrogen bonds (Figure 6) [49, 50]. Although the created interactions work synergistically and create rather similar nanofibers, defined hierarchies are not created by these materials.

Confining aggregation of supramolecular polymers requires strong but orthogonal interactions. In aqueous environments, amphiphilic interactions can provide such a strong confining force that does not necessarily interfere with the supramolecular polymerization. In general, amphiphilic molecules comprising polar head groups and hydrophobic groups, mostly aliphatic chains, can self-assemble into a variety of different nanostructures such as for example, spheres, vesicles, cylindrical micelles or bilayers, as shown in the following Figure 7. The aggregate structure can be predicted from the packing parameter p according to Israelachvili which is described as follows:

$$p = \frac{V_0}{A * l}$$

where V_0 is the volume of the hydrophobic group, l is the length of the aliphatic chain and A_0 is the surface area of the polar head group. As a consequence, the structure can be spherical ($p \leq 1/3$), cylindrical ($1/3 \leq p \leq 1/2$), vesicular ($1/2 \leq p \leq 1$) and lamellar ($p = 1$) [51]. According to its direct proportionality, an increase in for example the volume of the hydrophobic group will result in a transition from spherical structures towards cylindrical or vesicular/lamellar aggregates.

The morphology is mostly decided by the composition of the amphiphilic molecules, that is, the ratio of head group size compared to the length and volume of the aliphatic chains [24]. The diameter of the micelle or bilayer remains typically in the range of a few nanometers in the case of small molecules. If amphiphilic polymers are used, the dimensions can be further extended, but control over the formation of specific morphologies becomes far more challenging since interactions are more complex. Combining this amphiphilic assembly with supramolecular polymerization creates intriguing synergies that are related to their orthogonal character. In particular, if strong hydrogen bonds form the supramolecular polymer and the additional amphiphilic character does not interfere with the hydrogen bonding, hierarchical structures can be created. In such cases, amphiphilic molecular building blocks form supramolecular stacks driven by hydrogen bonding and/or π-π interactions, whereas hydrophobic interactions enable controlled

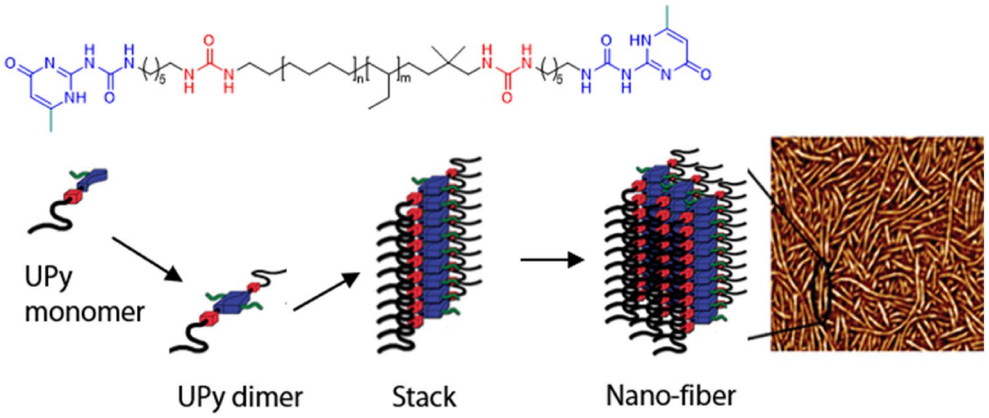

FIGURE 6 | Schematic representation of the theoretical aggregation of the end groups of UPy (blue) urea (red)-modified polymers into nanofibers. Adapted with permission [48]. © 1996 Royal Society of Chemistry. The UPy substituent at the six-position is depicted in green.

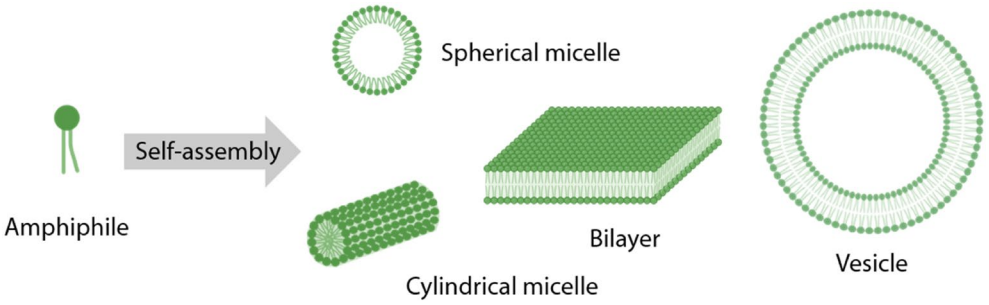

FIGURE 7 | Self-assembly of amphiphilic molecules into various kinds of nanostructures. Created with BioRender.

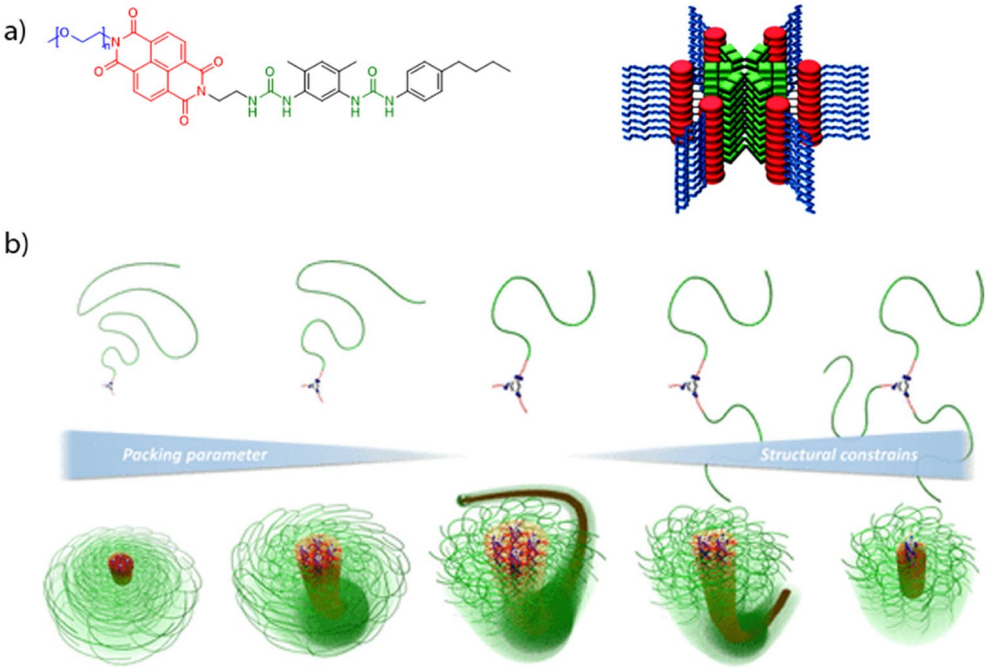

FIGURE 8 | Possible model for the self-assembly of PEO-NDI-U_2 in water into supramolecular cylinders via hydrogen bonds reinforced by hydrophobic interactions (a). Adapted with permission [49]. Copyright © 2011 American Chemical Society. Schematic depiction of the different assembly behavior (bottom) observed for the tested BTUs (top), which is influenced by either the structural arrangement of the hydrophilic polymer chains (right) or the packing parameter (left) (b). Reprinted with permission [52]. Copyright © 2020 American Chemical Society.

lateral aggregation. An example that nicely exemplifies the concept is *N*-substituted naphthalene diimides containing both a hydrophilic poly(ethylene glycol) chain (PEG) and a bisurea modified alkyl chain (PEG-NDI-U_2). These amphiphilic materials aggregate into 300 nm long and 13 nm wide nanorods, which are composed of about 6 molecules per cross-section in a star-shaped arrangement (Figure 8a) [48]. When substituted at the imide, the H bonding moieties will be oriented perpendicularly to the NDI plane, resulting in stronger H-bonding participation and facilitating superstructure formation [53]. Alternating sequences, as for example achieved by co-assembly of electron rich and electron poor stacks, provide additional control over the distribution of functionalities along the nanocylinder surface [54]. Similarly, bis(squaramide)s or amphiphilic urea derivatives assemble into long and highly anisotropic fibers or rigid filaments, respectively, carrying long aliphatic chains shielding the central supramolecular motif and inducing lateral aggregation in an aqueous environment, which is then counteracted by the attached hydrophilic polymer chains [55, 56]. While fiber formation is enforced by supramolecular stacking, the ratio of hydrophobic to hydrophilic groups decides the dimensions of the lateral aggregation, but it may also induce further morphology changes. For instance, increasing the length of the hydrophilic polymer chains in the case of an amphiphilic perylene bisimide motif leads to a transition from 2D towards 1D nanostructures, which is related to an increase in steric demands and thus, hindered lateral aggregation [57]. That dimensions can be rather well controlled, as illustrated by supramolecular systems based on amphiphilic polymers that comprise benzene trisureas (BTU) or trispeptides (BTP) as a central stacking motif. These central motifs are modified with three aliphatic chains creating a hydrophobic core unit, where one chain is further extended with a hydrophilic polymer chain. In water, these building blocks self-assemble into cylindrical micelles with defined diameters of 7–10 nm depending on the lateral aggregation of two or four columnar stacks [52, 58, 59]. Increasing the polymer length mainly impedes stacking into columnar structures due to an increased steric demand of the polymer chains, while the core size remains constant. Varying the amphiphilic structure by attaching additional hydrophilic polymers to the other aliphatic chains, however, prevents the lateral aggregation in addition to the impeded stacking of the columns (Figure 8b). The latter can still be enforced through introducing additional hydrogen bond forming groups [60].

Sufficient strong hydrogen bonding interactions even enable directing the self-assembly of amphiphilic block copolymers into a hierarchical cylindrical structure. This has been demonstrated using asymmetrically substituted cyclic peptides composed of alternating D- and L-amino acids, which form large tubes by antiparallel β-sheet-like stacking [61, 62]. Bearing a hydrophilic and a hydrophobic polymer chain, the tubes are formed at the interface of a cylindrical block copolymer micelle, leading not only to the name tubisomes, but also providing a more defined cylindrical structure (Figure 9) [63].

The case of cyclic peptides conjugated to amphiphilic polymers nicely exemplifies the potential of combining strong hydrogen-bonding units with amphiphilic properties to enhance the stability of supramolecular assemblies [64]. While the conjugation of hydrophilic polymers results in a dynamic system that is susceptible to disintegration upon dilution, the insertion of a hydrophobic block hinders dynamic exchange, making the structures resistant to dilution [65].

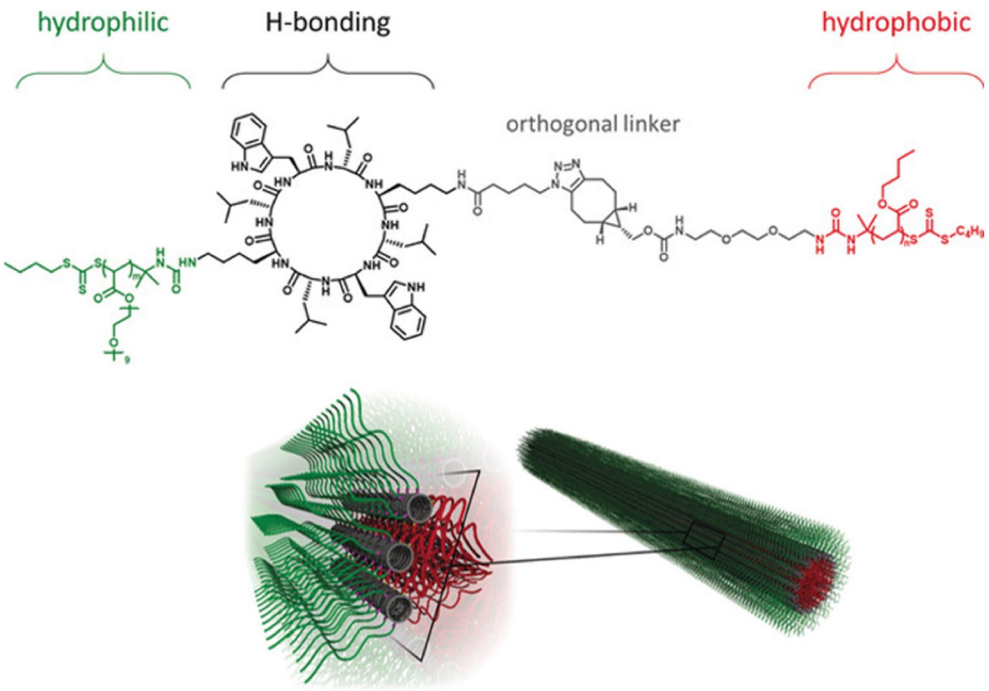

FIGURE 9 | Structure of the amphiphilic cyclic peptide/polymer conjugate p(butyl acrylate)-cyclic peptide-p(poly(ethylene glycol) acrylate) (top) and the self-assembly into tubisomes (bottom). Reprinted with permission [63]. Copyright © 2018 Wiley-VCH Verlag GmbH & Co. KGaA.

All these examples demonstrate the potential of synergistically applied orthogonal interactions to expand the scope of supramolecular polymerizations towards hierarchical structures with defined dimensions. Ideally, these dimensions can independently be controlled by adjusting the secondary interactions or by the ratio of peripheral to central groups, as it is exemplified by the hydrophilic/hydrophobic ratio in amphiphilic molecules. What remains to be explored is the incorporation of dedicated interactions in the periphery or the surface of these structures, which ultimately allows for expanding the levels of hierarchy similar to nature.

4 | Potential and Perspective of Tailored Hierarchical Superstructures

Several conceptual approaches towards hierarchical superstructures have been extensively described and discussed in literature. As a consequence, hierarchical superstructures defined at all scales are now probably on their advent, allowing to realize and control supramolecular nanostructures with tailored functionalities. This broad occurrence and their versatility implicate a countless number of opportunities and applications, which are related to the plethora of functional building blocks but more importantly to the structures' shape as well as to the surface interactions. In particular, superstructures with supramolecular chirality and their perspective have been recently extensively reviewed [25, 26]. This includes promising applications directly related to their chirality, for instance, in chiral recognition and sensing, chiroptical switches, and chiral or asymmetric catalysis. In the following, we focus on selected potential applications that are related to the defined hierarchical structure and precise positioning of functions, for which nature provides an excellent role model or has intriguing similarities.

Light-weight materials with tailored mechanics and functionality: As a first example, we briefly like to introduce macroscopic hierarchical structures which enhance mechanical properties and were developed by humankind centuries ago, namely yarn and ropes. Their structure has remarkable morphological similarities to natural fibers and helical fibers as outlined in the introduction and in Section 2. Natural fiber sources for yarn fabrication often rely on wool (protein-based fibers) or cotton (cellulose-based fibers). Both are essentially staple fibers, which means they have a finite length in contrast to synthetic polymer processed filaments. Cotton fibers are twisted ribbons with lengths in the cm range (Figure 10a) [66]. To produce a yarn of infinite length, these short fibers were spun and twisted in a way that the established entanglements between the staple fibers hamper slipping, which foster and improve the mechanical properties within the hierarchical structure. Several yarns can be further twisted to form strands and twisting of several strands in the opposite direction yields ropes [73]. In contrast to non-structured bulk materials, yarns and ropes with their lower density combine strength and toughness with excellent flexibility.

In particular, when realizing structural components with outstanding, though mechanical characteristics, nature uses hierarchically structured nanocomposites ranging from the nanoscopic to the macroscopic scale. In bones, these are based on nanoplatelets of hydroxyapatite within collagen fibrils (Figure 1). Apart from these bulk-type, fibrous hierarchical composites, nature uses also laminated plate-like structures with a prominent example being nacre [4]. Nacre is a hierarchical structure resembling a 'brick-and-mortar' morphology based on micron-sized ridged platelets of aragonite ($CaCO_3$) laminated with a small amount of proteins and polysaccharides [74]. This leads not only to an extraordinary stiffness and

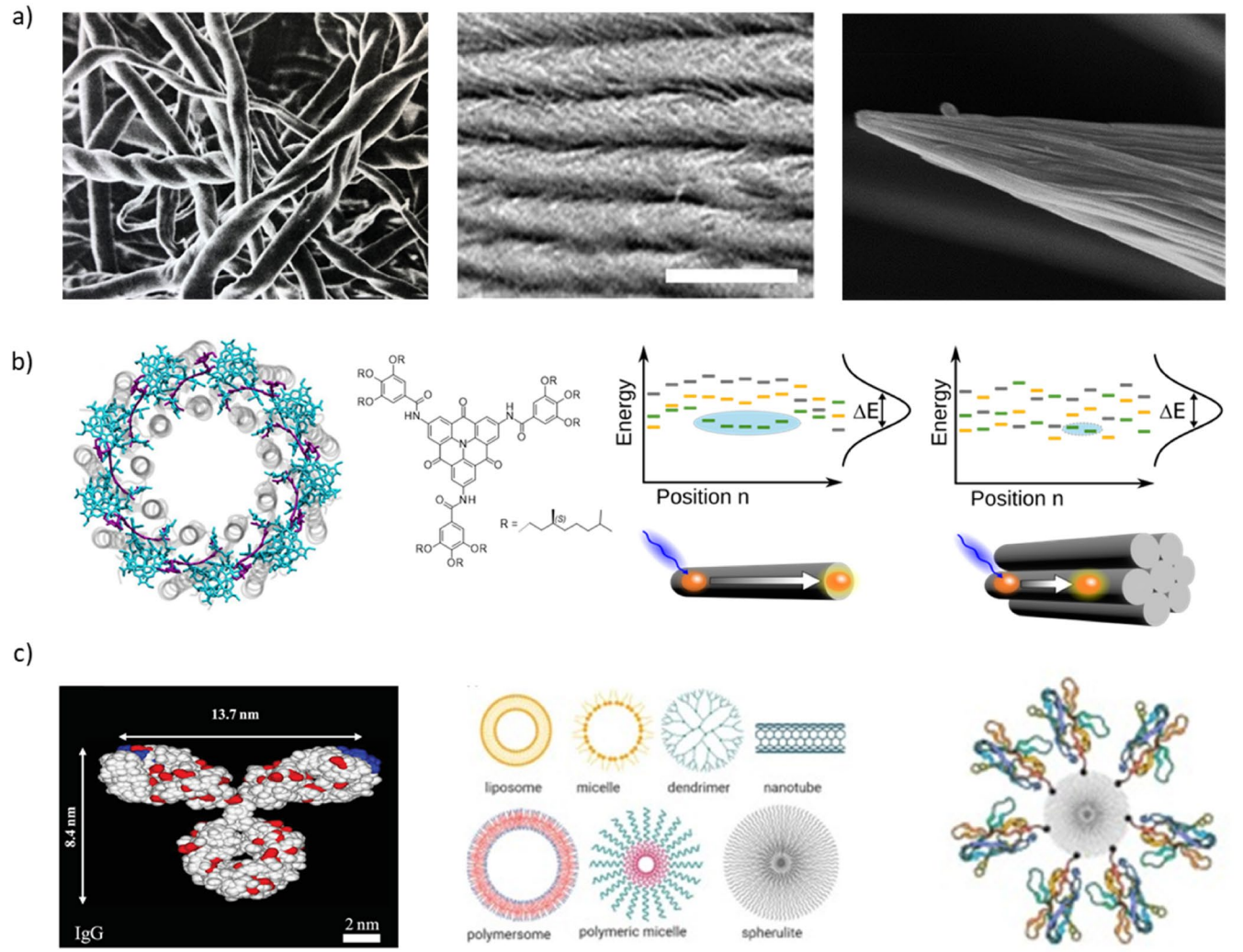

FIGURE 10 | Natural and artificial hierarchical structures. (a) SEM images of twisted ribbons of cotton fibers (left) [66], cross-section of cellulose nanocrystals/xylan composite film (middle) [67], and of BTA-based supramolecular spine (right) [68]. Adapted with permission [66]. Copyright 2007, Elsevier Ltd. Reprinted with permission [67]. Copyright © 2020, Wiley-VCH GmbH. Reprinted under the terms of the CC-BY license with permission [68]. Copyright © 2024, The Authors. Advanced Materials Interfaces published by Wiley-VCH GmbH. (b) LH II antenna complex of *Rhodoblastus acidophilus* (left) [69], chemical structure of a carbonyl-bridged triarylamine trisamide (CBT) (middle), single fibers and fiber bundles of CBTs showing differences in the excited state energy landscape (right) [70]. Adapted under the terms of the CC-BY 4.0 license with permission [69]. Copyright © 2021, The Authors, published by MDPI. Adapted under the terms of the CC-BY-NC-ND license with permission [70]. Copyright © 2020, The Authors, published by the American Chemical Society. (c) Dimensions and shape of antibody IgG (left) [71], potential types of aggregates for an artificial antibody (middle) [72], and an example containing 7 antigen binding sites in the periphery (right) [72]. Reprinted with permission [71]. Copyright © 2008, American Chemical Society. Adapted with permission [72]. Copyright © 2021, Elsevier Ltd.

strength related to the hard material aragonite but also to a high toughness related to the organic material and allows for energy dissipation [1, 4]. Consequently, there is a significant interest in mimicking this kind of hierarchical structure not only because of the mechanical properties but also due to appealing iridescent or transparent properties [75, 76]. A similar combination of properties, that is, tunable mechanical strength and iridescence can also be realized by combining cellulose nanocrystals and polysaccharides [67]. Upon evaporation induced self-assembly, this leads to thin hierarchically-structured films with chiral organization (Figure 10a). In all these cases, the functionality and properties are closely related to the tailored sequence of interacting interfaces within the bulk of the hierarchical nanocomposites.

The surface of hierarchical materials can also provide specific functionality. In other words, hierarchy can lead to surface structuring of objects that ultimately result in or enhance functionality. A prominent example are cacti spines. Certain species of cacti survive in arid regions without rainfall by harvesting atmospheric water with the help of their spines to ensure their water demand [77]. Cacti spines mainly consist of cellulose and other polysaccharides and feature a hierarchical fibrous structure [78–80]. Importantly in distinct species, the cacti spines surface is characterized by several features [77]. This includes their conical shape, which leads to a Laplace pressure difference. Together with the longitudinal micro-grooved surface, this facilitates water transport unidirectionally from their tip to their base even against gravity. The structure of the

microgrooves becomes smaller from the base to the tip, which additionally establishes a wettability gradient along the microgrooves. Artificial supramolecular cacti spines can be prepared by applying sophisticated self-assembly protocols using distinct BTAs [68]. These supramolecular spines with hierarchical structure contain all these elements (Figure 10a). Consequently, the surface of these supramolecular spines is able to unidirectionally transport water with a transport speed that even exceeds cacti spines of *O. microdasys* by a factor of ten.

Based on all these examples outlined above, one is tempted to say that the function, which results from hierarchy in bulk or is present on the surface on the micro- and macroscopic scale, is more a question of establishing and controlling the self-assembly procedures than of developing new classes of materials. However, controlling the solid-state morphology is an underestimated key property to tune mechanical characteristics and other properties, as nature has already impressively demonstrated with just a few building blocks (see Figure 1). Similarly, and as shown above, artificial nacre-like nanocomposites using established materials and preparation techniques have great potential for large-scale applications such as protective structures for panels, windows, and electronic housings [76].

Light harvesting, nanophotonics and electronics: One of nature's success stories is the design and evolution of photosynthetic machinery that effectively converts sunlight into a useful form of chemical energy [81]. One fascinating aspect is that photosynthetic organisms also function in extreme environments with low levels of sunlight. For example, green sulfur bacteria survive at sea depths of around 80 m with solar irradiation that is 14 orders of magnitude lower than on the surface [82, 83]. Thus, photons have to be absorbed, transported and used very efficiently. The initial steps of photosynthesis involve light-harvesting (absorption) and transport of excitation energy through their antenna systems before reaction takes place in the transducer. An outstanding feature is that exciton energy transport proceeds in a directed manner over distances of more than 100 nm and sometimes of up to 2 μm with a quantum efficiency close to unity [83–85]. Nature realizes this by using ensembles of superstructures, which create precisely arranged pigment-protein complexes. For example, the natural light-harvesting antenna complex II (LH II) represents a circular structure, in which 9 α-apoproteins are forming the inner wall and 9 β-apoproteins form the outer wall (Figure 10b) [86]. Between these proteins, a series of chromophores, that is, bacteriochlorophylls and carotenoids are precisely arranged leading to defined electronic Coulomb interactions between the chromophores. Their arrangement and interactions establish a defined excited-state energy landscape, which results in exciton delocalization and promotes coherent energy transport [83]. Equally important, the excited-state energy landscape features an intrinsic gradient that directs the diffusion of energy through the superstructure's ensemble although largely the same chromophores are used [81, 87].

Inspired by the unmatched properties of the natural photosynthetic machinery, several research groups have aimed to create artificial counterparts—particularly in view of exciton transport—based on chromophoric supramolecular systems. Similar to natural chromophores, linear, disk- or board-shaped chromophores are employed. These include, for example, polymethines or related dyes such as cyanines, merocyanines as well as squaraines or fused aromatic compounds such as naphthalene diimides, perylene bisimides, carbonyl-bridged triarylamines, porphyrins and hexabenzocoronenes [82]. In these compounds, self-assembly is driven by π-π stacking, but also supported by H-bonding, donor-acceptor (D-A) interactions or others. Depending on the molecular design, this leads to H aggregates (with a face-to-face arrangement), J aggregates (with a slipped-of arrangement) or aggregates with charge transfer (CT) character. Depending on the aggregate type, this has significant impact on the photophysics, including absorption, photoluminescence, life-time of the excited state, electronic coupling and ultimately energy transport. Research on supramolecular objects for light harvesting or exciton energy transport focusses on both supramolecular polymers as well as superstructures, including single- or multi-walled vesicles or micelles [88, 89], nanotubes [90–95] and Y-shaped nanotubes [96], as well as single nanofibers [70, 97], and nanofiber bundles. However, changing, for example, from a single nanofiber and nanofiber bundles, that is, from a supramolecular polymer to a structure with higher level, unavoidably introduces structural and electronic disorder (Figure 10b) [70, 97]. Both leads to exciton localization and reduces exciton energy transport. On the other hand, if disorder is implemented in a controlled manner, this allows to build-up an energy gradient in superstructures [98].

To mimic and/or implement chromophoric superstructures, however, holds great promise and leads to improved properties of existing technologies or to novel applications. For instance, a limiting factor in bulk heterojunction solar cells is the incoherent exciton hopping after light absorption, which proceeds only over a distance of a few tenths of nm. As a result, the excitons cannot always reach the donor-acceptor interface required for charge separation. Efficient transport of exciton energy between the interfaces therefore reduces one of the loss channels. Chromophoric superstructures on the nanoscale also have the potential to be used in nanophotonics and in excitonic circuits [99, 100]. In particular, the latter requires significant spatial control and manipulation of the supramolecular objects. Coherence in chromophoric superstructures is not only relevant for long-range energy transport, but may have the potential in the field of quantum information science and technology [82, 101]. If, for example, a single molecule is regarded as a qubit (quantum bit), supramolecular systems can be considered as arrangements of qubits if there is sufficiently strong electronic coupling between the individual building blocks to promote entanglement [102]. All these applications can be achieved with thermodynamically stable or static supramolecular polymers or superstructures. A potentially exciting application, which in contrast requires an adaptive system, may be neuromorphic computing with supramolecular objects. Neuromorphic computing relies on a dense network of interconnected "neurons", which operate in a parallel fashion [103, 104]. Learning and training the memory is related to the connectivity, which can be regarded as wiring, between neurons. In this context, the dynamic and reversible nature of supramolecular systems may be employed to foster, re-establish, or unplug such connections between artificial neurons.

Strict guidelines for the molecular design of efficient chromophoric supramolecular polymers and superstructures for various purposes have not been established by now. This is evidenced by

the small number of known artificial systems that exhibit exceptional long-range energy transport (> 100 nm) [97]. Even in supramolecular assemblies based on the same building blocks, significant variations in energy transport can be detected, which can theoretically be described by a kind of disorder, although the origin is unknown [105]. To gain a deeper understanding, dedicated model compounds and controlled self-assembly procedures are required, supported by structural elucidation using state-of-the-art analytical techniques. Disorder is not only related to potential defects in the chromophore structure but also to the periphery. It can be assumed that soft and rigid, polar and non-polar structures, among others, influence the photophysics of self-assembled chromophores. For a more comprehensive understanding and to unleash the potential, further tailored chromophoric systems in combination with defined structure-directing supramolecular motifs are required. This is particularly relevant to broaden the theoretical and experimental understanding between the H and J aggregates and structures with CT states [82, 106]. Equally important is the electronic coupling between the chromophores, which depends on the chromophore and the non-covalent interactions regulating the position of those to each other. The electronic coupling determines the delocalization of the excitons, which typically includes only a couple of chromophores [107]. This ultimately has an impact on the coherent transport properties and therefore on the efficiency and purpose.

Artificial antibodies and targeted nanomedicine: Apart from the photosynthetic machinery or enzymes, which both are able to perform chemical reactions, antibodies are another remarkable approach of nature that is based on the formation of a defined superstructure. In particular, antibodies represent the primary weapon in defense of complex organisms and enable them to counteract any pathogen such as viruses or bacteria. For instance, the human adaptive immune system can quickly release neutralizing antibodies when infections with viral pathogens reoccur or adapt them to mutated but closely related pathogens [108]. However, in the case of newly emerging and highly contagious pathogens—as exemplified by the recent severe acute respiratory syndrome coronavirus 2 (SARS-CoV-2) – it takes about several days to weeks to identify and produce efficient antibodies that can neutralize the viral thread [109]. This delay in the immune response, however, exacerbates the effects of these pathogens, which can lead to severe disease progression and result in immediate or premature death and also contributes to the spread of the virus.

Antibodies generally belong to the family of immunoglobulins (Ig). Immunoglobulins are composed of proteins with a precise and distinct sequence of amino acids, with the most prominent example being the IgG. The IgG represents the "monomeric" form of antibodies and consists of two identical so-called 'heavy chain' polypeptides and two identical so-called 'light chain' polypeptides. These chains are arranged by inter- and intramolecular non-covalent interactions and four disulfide bridges into the prominent Y-shaped superstructure (Figure 10c) [110]. This Y-shaped superstructure weighs approx. 150 kDa, has a length of approx. 9 nm and a width of approx. 14 nm, the latter being the distance between the two antigen binding sites (epitopes) on the tip of the "Y" [71]. Another important representative of antibodies is the IgM, which corresponds to the pentameric form with 10 antigen binding sites and a weight of about 900 kDa. Antibodies such as IgG are anisotropic and significantly larger than simple (macro)molecules, but also significantly smaller than viruses with a diameter in the range of 100 nm. Therefore, several IgGs are involved in forming antibody-virus complexes and their neutralization activity requires a relatively high affinity of the antibody for exposed structures on the viral surface [111, 112]. An interesting feature of released antibodies, which are produced and/or stored from naïve or memory B cells, is that they are stable in their environment for at least days to weeks demonstrating an intrinsic and significant thermodynamic stability.

In view of a possible emerging pandemic in the future, it is becoming clear that artificial antibodies that bind effectively to virus capsids could play a pivotal role in preventing damage to health and the spread of the virus. Well-investigated approaches focus on the biosynthetic production of antibodies, which can be applied in the field of antibody therapies [113]. Commonly pursued biotechnological-based approaches include so-called monoclonal antibodies and recombinant antibodies. Monoclonal antibodies are obtained by harvesting B cells from virus-infected species and combining them with specific cell lines that produce the antibody. Recombinant antibodies are achieved by fusing the genetic information for antibody production with the viral genome of bacteriophages, which then express the antibody (fragment) on their surface [114]. Both the monoclonal and the recombinant antibodies have in common that the artificial antibodies feature similar or the same stability with corresponding nanoscopic shape and dimensions and specific antigen binding sites (epitopes). However, their preparation is time-consuming and requires sophisticated work-up and purification procedures rendering the production costs high. Thus, synthetic approaches that comprise various self-assembly strategies may represent a promising alternative. Nanosized objects may be based on, for example, liposomes, polymersomes, micelles, polymer micelles, dendritic or tubular structures, which bear the epitopes on the structures' surface (Figure 10c) [72]. These epitopes may be based on sialic acids or other protein fragments, which are suitable for virus neutralization by establishing superstructure-virus interactions via hydrogen bonding, salt/ionic bridges as well as van der Waals interactions. At the current stage, it remains a challenge to create real artificial antibodies with similar efficacy. We anticipate that an ideal superstructure should fulfill various requirements, as for example that the dimensions should be similar in the range of IgG or IgM to match viral sizes and distances of target domains. Realizing such structures requires dimensional control beyond single molecules, polymer chains, or even conventional self-assemblies. Combinations of orthogonal supramolecular motifs might, however, achieve the required structural control. Nevertheless, their structural stability and integrity in biological environments must be ensured, which requires, in addition, a high stability of the self-assembled hierarchical structures. This also includes extremely diluted conditions excluding systems that are in a dynamic equilibrium between self-assembly and disassembly. So far, only very few systems have been analyzed for stability under such diluted conditions, which must be addressed in future if such applications are considered. The most promising candidates in this regard appear to be systems that combine orthogonal interactions such as strong hydrogen bonds and an amphiphilic character. In advanced nanomedicine, high affinities of the epitopes towards

specific targets are further desired for tailored therapeutic approaches, which can be compensated by multivalency in the case of weak individual interactions. However, high charge densities or highly interacting epitopes can affect the biocompatibility of synthetic systems and cause undesired immune responses, which probably limits their use to topical applications.

5 | Conclusion

Nature has generated numerous fascinating models by constructing defined superstructures with tailored functionalities that are often the result of the different hierarchical levels across multiple length scales rather than the property of the individual building blocks. Following this approach, the production and use of artificial systems depend crucially on control over the dimensional shape. Defined superstructure formation across the hierarchical levels can be achieved by precisely controlling and directing the self-assembly process leading to nanocomposites or tailored mesoscale structures with functionalities that are encoded in the bulk or imprinted in the surface of the objects. Yet the ultimate control of defined superstructures on the nanoscale is probably more likely to be achieved by combining non-covalent interactions in an orthogonal manner, for example, through hydrogen bonding and amphiphilic interactions, or confinement by packing restrictions as demonstrated for many chiral compounds. This undoubtedly enables countless combinations to realize a variety of defined objects with hierarchical structure bridging from the nano- to the meso- and maybe even to the macro-scale. But more appreciably, a suitable design and the tailored introduction of specific functionalities will enable the creation of unprecedented materials, such as multiphotochromic systems or adaptive antibody-like structures, with exceptional properties and unmatched features.

Acknowledgments

The authors thank the German Science Foundation (DFG) for generous funding within the Heisenberg-Programme (Project-ID: 517761335).

References

1. U. G. K. Wegst, H. Bai, E. Saiz, A. P. Tomsia, and R. O. Ritchie, "Bioinspired Structural Materials," *Nature Materials* 14 (2015): 23–36.

2. T. Misteli, "The Concept of Self-Organization in Cellular Architecture," *Journal of Cell Biology* 155 (2001): 181–185.

3. A. Gautieri, S. Vesentini, A. Redaelli, and M. J. Buehler, "Hierarchical Structure and Nanomechanics of Collagen Microfibrils From the Atomistic Scale Up," *Nano Letters* 11 (2011): 757–766.

4. D. Nepal, S. Kang, K. M. Adstedt, et al., "Hierarchically Structured Bioinspired Nanocomposites," *Nature Materials* 22 (2023): 18–35.

5. R. Lakes, "Materials With Structural Hierarchy," *Nature* 361 (1993): 511–515.

6. U. G. K. Wegst, "Bending Efficiency Through Property Gradients in Bamboo, Palm, and Wood-Based Composites," *Journal of the Mechanical Behavior of Biomedical Materials* 4 (2011): 744–755.

7. H.-W. Schmidt and F. Würthner, "A Periodic System of Supramolecular Elements," *Angewandte Chemie, International Edition* 59 (2020): 8766–8775.

8. J. W. Steed and J. L. Atwood, *Supramolecular Chemistry* (Wiley, 2009).

9. L. Brunsveld, B. J. B. Folmer, E. W. Meijer, and R. P. Sijbesma, "Supramolecular Polymers," *Chemical Reviews* 101 (2001): 4071–4098.

10. T. F. A. De Greef, M. M. J. Smulders, M. Wolffs, A. P. H. J. Schenning, R. P. Sijbesma, and E. W. Meijer, "Supramolecular Polymerization," *Chemical Reviews* 109 (2009): 5687–5754.

11. T. Aida, E. W. Meijer, and S. I. Stupp, "Functional Supramolecular Polymers," *Science* 335 (2012): 813–817.

12. T. D. Clemons and S. I. Stupp, "Design of Materials With Supramolecular Polymers," *Progress in Polymer Science* 111 (2020): 101310.

13. G. M. Whitesides and B. Grzybowski, "Self-Assembly at all Scales," *Science* 295 (2002): 2418–2421.

14. M. Wehner and F. Würthner, "Supramolecular Polymerization Through Kinetic Pathway Control and Living Chain Growth," *Nature Reviews Chemistry* 4 (2020): 38–53.

15. S. Cantekin, T. F. A. de Greef, and A. R. A. Palmans, "Benzene-1,3,5-Tricarboxamide: A Versatile Ordering Moiety for Supramolecular Chemistry," *Chemical Society Reviews* 41 (2012): 6125–6137.

16. M. P. Lightfoot, F. S. Mair, R. G. Pritchard, and J. E. Warren, "New Supramolecular Packing Motifs: π-Stacked Rods Encased in Triply-Helical Hydrogen Bonded Amide Strands," *Chemical Communications* (1999): 1945–1946.

17. C. M. A. Leenders, L. Albertazzi, T. Mes, M. M. E. Koenigs, A. R. A. Palmans, and E. W. Meijer, "Supramolecular Polymerization in Water Harnessing Both Hydrophobic Effects and Hydrogen Bond Formation," *Chemical Communications* 49 (2013): 1963–1965.

18. C. S. Zehe, J. A. Hill, N. P. Funnell, et al., "Mesoscale Polarization by Geometric Frustration in Columnar Supramolecular Crystals," *Angewandte Chemie, International Edition* 56 (2017): 4432–4437.

19. C. M. A. Leenders, M. B. Baker, I. A. B. Pijpers, et al., "Supramolecular Polymerisation in Water; Elucidating the Role of Hydrophobic and Hydrogen-Bond Interactions," *Soft Matter* 12 (2016): 2887–2893.

20. R. P. M. Lafleur, S. Herziger, S. M. C. Schoenmakers, et al., "Supramolecular Double Helices From Small C3-Symmetrical Molecules Aggregated in Water," *Journal of the American Chemical Society* 142 (2020): 17644–17652.

21. H. v. Berlepsch, K. Ludwig, B. Schade, R. Haag, and C. Böttcher, "Progress in the Direct Structural Characterization of Fibrous Amphiphilic Supramolecular Assemblies in Solution by Transmission Electron Microscopic Techniques," *Advances in Colloid and Interface Science* 208 (2014): 279–292.

22. M. B. Baker, L. Albertazzi, I. K. Voets, et al., "Consequences of Chirality on the Dynamics of a Water-Soluble Supramolecular Polymer," *Nature Communications* 6 (2015): 6234.

23. X. Lou, R. P. M. Lafleur, C. M. A. Leenders, et al., "Dynamic Diversity of Synthetic Supramolecular Polymers in Water as Revealed by Hydrogen/Deuterium Exchange," *Nature Communications* 8 (2017): 15420.

24. J. N. Israelachvili, *Intermolecular and Surface Forces*, 2nd ed. (Academic Press, 2007).

25. M. Liu, L. Zhang, and T. Wang, "Supramolecular Chirality in Self-Assembled Systems," *Chemical Reviews* 115 (2015): 7304–7397.

26. Y. Sang and M. Liu, "Hierarchical Self-Assembly Into Chiral Nanostructures," *Chemical Science* 13 (2022): 633–656.

27. G. Albano, G. Pescitelli, and L. Di Bari, "Chiroptical Properties in Thin Films of π-Conjugated Systems," *Chemical Reviews* 120 (2020): 10145–10243.

28. R. S. Cahn, C. Ingold, and V. Prelog, "Specification of Molecular Chirality," *Angewandte Chemie, International Edition in English* 5 (1966): 385–415.

29. A. R. A. Palmans and E. W. Meijer, "Amplification of Chirality in Dynamic Supramolecular Aggregates," *Angewandte Chemie International Edition* 46 (2007): 8948–8968.

30. J. van Gestel, A. R. A. Palmans, B. Titulaer, J. A. J. M. Vekemans, and E. W. Meijer, ""Majority-Rules" Operative in Chiral Columnar Stacks ofC3-Symmetrical Molecules," *Journal of the American Chemical Society* 127 (2005): 5490–5494.

31. A. J. Wilson, J. van Gestel, R. P. Sijbesma, and E. W. Meijer, "Amplification of Chirality in Benzene Tricarboxamide Helical Supramolecular Polymers," *Chemical Communications* (2006): 4404–4406.

32. M. M. J. Smulders, A. P. H. J. Schenning, and E. W. Meijer, "Insight Into the Mechanisms of Cooperative Self-Assembly: The "Sergeants-and-Soldiers" Principle of Chiral and Achiral C3-Symmetrical Discotic Triamides," *Journal of the American Chemical Society* 130 (2008): 606–611.

33. L. Brunsveld, B. G. G. Lohmeijer, J. A. J. M. Vekemans, and E. W. Meijer, "Chirality Amplification in Dynamic Helical Columns in Water," *Chemical Communications* (2000): 2305–2306.

34. A. R. A. Palmans, J. A. J. M. Vekemans, E. E. Havinga, and E. W. Meijer, "Sergeants-and-Soldiers Principle in Chiral Columnar Stacks of Disc-Shaped Molecules withC3Symmetry," *Angewandte Chemie, International Edition in English* 36 (1997): 2648–2651.

35. F. V. de Graaf, C. Zoister, B. Schade, et al., "Amplification of Asymmetry via Structural Transitions in Supramolecular Polymer–Surfactant Coassemblies," *Journal of the American Chemical Society* 147 (2025): 17468–17476.

36. J. M. Ribó, J. Crusats, F. Sagués, J. Claret, and R. Rubires, "Chiral Sign Induction by Vortices During the Formation of Mesophases in Stirred Solutions," *Science* 292 (2001): 2063–2066.

37. E. Yashima, N. Ousaka, D. Taura, K. Shimomura, T. Ikai, and K. Maeda, "Supramolecular Helical Systems: Helical Assemblies of Small Molecules, Foldamers, and Polymers With Chiral Amplification and Their Functions," *Chemical Reviews* 116 (2016): 13752–13990.

38. L. A. Estroff and A. D. Hamilton, "Water Gelation by Small Organic Molecules," *Chemical Reviews* 104 (2004): 1201–1218.

39. P. Terech and R. H. Wade, "The Relationship Between a Dried and Native Steroid Gel," *Journal of Colloid and Interface Science* 125 (1988): 542–551.

40. A. Ajayaghosh, R. Varghese, S. J. George, and C. Vijayakumar, "Transcription and Amplification of Molecular Chirality to Oppositely Biased Supramolecular π Helices," *Angewandte Chemie, International Edition* 45 (2006): 1141–1144.

41. P. P. Bose, M. G. B. Drew, A. K. Das, and A. Banerjee, "Formation of Triple Helical Nanofibers Using Self-Assembling Chiral Benzene-1,3,5-Tricarboxamides and Reversal of the Nanostructure's Handedness Using Mirror Image Building Blocks," *Chemical Communications* (2006): 3196–3198.

42. P. Terech and R. G. Weiss, "Low Molecular Mass Gelators of Organic Liquids and the Properties of Their Gels," *Chemical Reviews* 97 (1997): 3133–3160.

43. R. H. Wade, P. Terech, E. A. Hewat, R. Ramasseul, and F. Volino, "The Network Structure of a Steroid/Cyclohexane Physical Gel," *Journal of Colloid and Interface Science* 114 (1986): 442–451.

44. A. Thierry, C. Straupé, B. Lotz, and J. C. Wittmann, "Physical Gelation: A Path Towards Ideal Dispersion of Additives in Polymers," *Polymer Communications* 31 (1990): 299–301.

45. J. Li, K. Fan, X. Guan, Y. Yu, and J. Song, "Self-Assembly Mechanism of 1,3:2,4-Di(3,4-Dichlorobenzylidene)-d-Sorbitol and Control of the Supramolecular Chirality," *Langmuir* 30 (2014): 13422–13429.

46. S. J. George, A. Ajayaghosh, P. Jonkheijm, A. P. H. J. Schenning, and E. W. Meijer, "Coiled-Coil Gel Nanostructures of Oligo(p-Phenylenevinylene)s: Gelation-Induced Helix Transition in a Higher-Order Supramolecular Self-Assembly of a Rigid π-Conjugated System," *Angewandte Chemie, International Edition* 43 (2004): 3422–3425.

47. J. Wu, J. Zhang, Y. Liu, et al., "Supramolecular Chiral Assembly of Symmetric Molecules With an Extended Conjugated Core," *ACS Applied Materials & Interfaces* 14 (2022): 33734–33745.

48. T. Choisnet, D. Canevet, M. Sallé, et al., "Robust Supramolecular Nanocylinders of Naphthalene Diimide in Water," *Chemical Communications* 55 (2019): 9519–9522.

49. W. P. J. Appel, G. Portale, E. Wisse, P. Y. W. Dankers, and E. W. Meijer, "Aggregation of Ureido-Pyrimidinone Supramolecular Thermoplastic Elastomers Into Nanofibers: A Kinetic Analysis," *Macromolecules* 44 (2011): 6776–6784.

50. A. J. P. Teunissen, M. M. L. Nieuwenhuizen, F. Rodríguez-Llansola, A. R. A. Palmans, and E. W. Meijer, "Mechanically Induced Gelation of a Kinetically Trapped Supramolecular Polymer," *Macromolecules* 47 (2014): 8429–8436.

51. J. N. Israelachvili, *Intermolecular and Surface Forces*, 2nd ed. (Academic Press, 1991).

52. F. V. Gruschwitz, M.-C. Fu, T. Klein, et al., "Unraveling Decisive Structural Parameters for the Self-Assembly of Supramolecular Polymer Bottlebrushes Based on Benzene Trisureas," *Macromolecules* 53 (2020): 7552–7560.

53. K. Gayen, S. Hazra, A. K. Pal, S. Paul, A. Datta, and A. Banerjee, "Tuning of the Optoelectronic Properties of Peptide-Appended Core-Substituted Naphthalenediimides: The Role of Self-Assembly of Two Positional Isomers," *Soft Matter* 17 (2021): 7168–7176.

54. T. Choisnet, D. Canevet, M. Sallé, et al., "Colored Janus Nanocylinders Driven by Supramolecular Coassembly of Donor and Acceptor Building Blocks," *ACS Nano* 15 (2021): 2569–2577.

55. V. Saez Talens, P. Englebienne, T. T. Trinh, W. E. M. Noteborn, I. K. Voets, and R. E. Kieltyka, "Aromatic Gain in a Supramolecular Polymer," *Angewandte Chemie, International Edition* 54 (2015): 10502–10506.

56. E. Obert, M. Bellot, L. Bouteiller, F. Andrioletti, C. Lehen-Ferrenbach, and F. Boué, "Both Water- and Organo-Soluble Supramolecular Polymer Stabilized by Hydrogen-Bonding and Hydrophobic Interactions," *Journal of the American Chemical Society* 129 (2007): 15601–15605.

57. S. Berruée, J.-M. Guigner, T. Bizien, L. Bouteiller, L. Sosa Vargas, and J. Rieger, "Spontaneous Formation of Polymeric Nanoribbons in Water Driven by π–π Interactions," *Angewandte Chemie, International Edition* 64 (2025): e202413627.

58. T. Klein, H. F. Ulrich, F. V. Gruschwitz, et al., "Impact of Amino Acids on the Aqueous Self-Assembly of Benzenetrispeptides Into Supramolecular Polymer Bottlebrushes," *Polymer Chemistry* 11 (2020): 6763–6771.

59. H. F. Ulrich, F. V. Gruschwitz, T. Klein, et al., "Influence of Polymer Side Chain Size and Backbone Length on the Self-Assembly of Supramolecular Polymer Bottlebrushes," *Chemistry - A European Journal* 30 (2024): e202400160.

60. T. Klein, H. F. Ulrich, F. V. Gruschwitz, et al., "Overcoming the Necessity of a Lateral Aggregation in the Formation of Supramolecular Polymer Bottlebrushes in Water," *Macromolecular Rapid Communications* 42 (2021): e2000585.

61. M. R. Ghadiri, J. R. Granja, R. A. Milligan, D. E. McRee, and N. Khazanovich, "Self-Assembling Organic Nanotubes Based on a Cyclic Peptide Architecture," *Nature* 366 (1993): 324–327.

62. J. Chen, Q. Li, P. Wu, et al., "Cyclic γ-Peptides With Transmembrane Water Channel Properties," *Frontiers in Chemistry* 8 (2020): 368.

63. J. C. Brendel, J. Sanchis, S. Catrouillet, et al., "Secondary Self-Assembly of Supramolecular Nanotubes Into Tubisomes and Their Activity on Cells," *Angewandte Chemie, International Edition* 57 (2018): 16678–16682.

64. J. Y. Rho, H. Cox, E. D. H. Mansfield, et al., "Dual Self-Assembly of Supramolecular Peptide Nanotubes to Provide Stabilisation in Water," *Nature Communications* 10 (2019): 4708.

65. M. Kariuki, J. Y. Rho, S. C. L. Hall, and S. Perrier, "Investigating the Impact of Hydrophobic Polymer Segments on the Self-Assembly Behavior of Supramolecular Cyclic Peptide Systems via Asymmetric-Flow Field Flow Fractionation," *Macromolecules* 56 (2023): 6618–6632.

66. I. M. Hutten, *Handbook of Nonwoven Filter Media* (Elsevier Science, 2007).

67. K. Adstedt, E. A. Popenov, K. J. Pierce, et al., "Chiral Cellulose Nanocrystals With Intercalated Amorphous Polysaccharides for Controlled Iridescence and Enhanced Mechanics," *Advanced Functional Materials* 30 (2020): 2003597.

68. M. Weber, F. Bretschneider, K. Kreger, A. Greiner, and H.-W. Schmidt, "Mimicking Cacti Spines via Hierarchical Self-Assembly for Water Collection and Unidirectional Transport," *Advanced Materials Interfaces* 11, no. 29 (2024): 2400101.

69. H. Lokstein, G. Renger, and J. P. Götze, "Photosynthetic Light-Harvesting (Antenna) Complexes—Structures and Functions," *Molecules* 26 (2021): 3378.

70. B. Wittmann, F. A. Wenzel, S. Wiesneth, et al., "Enhancing Long-Range Energy Transport in Supramolecular Architectures by Tailoring Coherence Properties," *Journal of the American Chemical Society* 142 (2020): 8323–8330.

71. Y. H. Tan, M. Liu, B. Nolting, J. G. Go, J. Gervay-Hague, and G.-y. Liu, "A Nanoengineering Approach for Investigation and Regulation of Protein Immobilization," *ACS Nano* 2 (2008): 2374–2384.

72. E. M. Obeng, C. K. O. Dzuvor, and M. K. Danquah, "Anti-SARS-CoV-1 and –2 Nanobody Engineering Towards Avidity-Inspired Therapeutics," *Nano Today* 42 (2022): 101350.

73. H.-J. Kolowski, *Chemiefaser-Lexikon*, 2nd ed. (Deutscher Fachverlag, 2009).

74. J. Sun and B. Bhushan, "Hierarchical Structure and Mechanical Properties of Nacre: A Review," *RSC Advances* 2, no. 20 (2012): 7617–7632.

75. F. Lossada, D. Jiao, D. Hoenders, and A. Walther, "Recyclable and Light-Adaptive Vitrimer-Based Nacre-Mimetic Nanocomposites," *ACS Nano* 15 (2021): 5043–5055.

76. Z. Yin, F. Hannard, and F. Barthelat, "Impact-Resistant Nacre-Like Transparent Materials," *Science* 364 (2019): 1260–1263.

77. J. Ju, H. Bai, Y. Zheng, T. Zhao, R. Fang, and L. Jiang, "A Multi-Structural and Multi-Functional Integrated Fog Collection System in Cactus," *Nature Communications* 3 (2012): 1247.

78. M. E. Malainine, A. Dufresne, D. Dupeyre, M. Mahrouz, R. Vuong, and M. R. Vignon, "Structure and Morphology of Cladodes and Spines of Opuntia Ficus-Indica. Cellulose Extraction and Characterisation," *Carbohydrate Polymers* 51 (2003): 77–83.

79. F. T. Malik, R. M. Clement, D. T. Gethin, et al., "Hierarchical Structures of Cactus Spines that Aid in the Directional Movement of Dew Droplets," *Philosophical Transactions of the Royal Society of London, Series A* 374 (2016): 20160110.

80. U. Schlegel, "The Composite Structure of Cactus Spines," *Bradleya* 2009 (2009): 129–138.

81. R. J. Cogdell, A. Gall, and J. Köhler, "The Architecture and Function of the Light-Harvesting Apparatus of Purple Bacteria: From Single Molecules to In Vivo Membranes," *Quarterly Reviews of Biophysics* 39 (2006): 227–324.

82. K. Kreger, H.-W. Schmidt, and R. Hildner, "Tailoring the Excited-State Energy Landscape in Supramolecular Nanostructures," *Electronic Structure* 3 (2021): 023001.

83. G. D. Scholes, G. R. Fleming, A. Olaya-Castro, and R. van Grondelle, "Lessons From Nature About Solar Light Harvesting," *Nature Chemistry* 3 (2011): 763–774.

84. X. Hu, T. Ritz, A. Damjanović, F. Autenrieth, and K. Schulten, "Photosynthetic Apparatus of Purple Bacteria," *Quarterly Reviews of Biophysics* 35 (2002): 1–62.

85. G. D. Scholes, G. R. Fleming, L. X. Chen, et al., "Using Coherence to Enhance Function in Chemical and Biophysical Systems," *Nature* 543 (2017): 647–656.

86. G. McDermott, S. M. Prince, A. A. Freer, et al., "Crystal Structure of an Integral Membrane Light-Harvesting Complex From Photosynthetic Bacteria," *Nature* 374 (1995): 517–521.

87. J. Strümpfer, M. Şener, and K. Schulten, "How Quantum Coherence Assists Photosynthetic Light-Harvesting," *Journal of Physical Chemistry Letters* 3 (2012): 536–542.

88. C. Li, J. Zhang, S. Zhang, and Y. Zhao, "Efficient Light-Harvesting Systems With Tunable Emission Through Controlled Precipitation in Confined Nanospace," *Angewandte Chemie, International Edition* 58 (2019): 1643–1647.

89. C. F. Calver, K. S. Schanze, and G. Cosa, "Biomimetic Light-Harvesting Antenna Based on the Self-Assembly of Conjugated Polyelectrolytes Embedded Within Lipid Membranes," *ACS Nano* 10 (2016): 10598–10605.

90. J. R. Caram, S. Doria, D. M. Eisele, et al., "Room-Temperature Micron-Scale Exciton Migration in a Stabilized Emissive Molecular Aggregate," *Nano Letters* 16 (2016): 6808–6815.

91. K. A. Clark, E. L. Krueger, and D. A. Vanden Bout, "Direct Measurement of Energy Migration in Supramolecular Carbocyanine Dye Nanotubes," *Journal of Physical Chemistry Letters* 5 (2014): 2274–2282.

92. Y. Wan, A. Stradomska, J. Knoester, and L. Huang, "Direct Imaging of Exciton Transport in Tubular Porphyrin Aggregates by Ultrafast Microscopy," *Journal of the American Chemical Society* 139 (2017): 7287–7293.

93. T. Kim, S. Ham, S. H. Lee, Y. Hong, and D. Kim, "Enhancement of Exciton Transport in Porphyrin Aggregate Nanostructures by Controlling the Hierarchical Self-Assembly," *Nanoscale* 10 (2018): 16438–16446.

94. A. P. Deshmukh, W. Zheng, C. Chuang, et al., "Near-Atomic-Resolution Structure of J-Aggregated Helical Light-Harvesting Nanotubes," *Nature Chemistry* 16 (2024): 800–808.

95. D. M. Eisele, D. H. Arias, X. Fu, et al., "Robust Excitons Inhabit Soft Supramolecular Nanotubes," *Proceedings. National Academy of Sciences. United States of America* 111 (2014): E3367–E3375.

96. C. Zoister, B. Schade, K. Ludwig, R. Haag, H. v. Berlepsch, and A. K. Singh, "Self-Assembly of a Perfluorinated Amphiphilic Cyanine Dye Into Branched Tubular J-Aggregates," *Chemistry-A European Journal* 31 (2025): e202403848.

97. A. T. Haedler, K. Kreger, A. Issac, et al., "Long-Range Energy Transport in Single Supramolecular Nanofibres at Room Temperature," *Nature* 523 (2015): 196–199.

98. S. Stäter, F. A. Wenzel, H. Welz, et al., "Directed Gradients in the Excited-State Energy Landscape of Poly(3-Hexylthiophene) Nanofibers," *Journal of the American Chemical Society* 145 (2023): 13780–13787.

99. H. Park, N. Heldman, P. Rebentrost, et al., "Enhanced Energy Transport in Genetically Engineered Excitonic Networks," *Nature Materials* 15 (2016): 211–216.

100. É. Boulais, N. P. D. Sawaya, R. Veneziano, et al., "Programmed Coherent Coupling in a Synthetic DNA-Based Excitonic Circuit," *Nature Materials* 17 (2018): 159–166.

101. M. R. Wasielewski, M. D. E. Forbes, N. L. Frank, et al., "Exploiting Chemistry and Molecular Systems for Quantum Information Science," *Nature Reviews Chemistry* 4 (2020): 490–504.

102. J. H. Reina, C. E. Susa, and R. Hildner, "Conditional Quantum Dynamics and Nonlocal States in Dimeric and Trimeric Arrays of Organic Molecules," *Physical Review A* 97 (2018): 063422.

103. Y. van de Burgt, A. Melianas, S. T. Keene, G. Malliaras, and A. Salleo, "Organic Electronics for Neuromorphic Computing," *Nature Electronics* 1 (2018): 386–397.

104. I. Valov and M. Kozicki, "Organic Memristors Come of Age," *Nature Materials* 16 (2017): 1170–1172.

105. A. Carta, B. Wittmann, K. Kreger, H.-W. Schmidt, T. L. C. Jansen, and R. Hildner, "Spatial Correlations Drive Long-Range Transport and Trapping of Excitons in Single H-Aggregates: Experiment and Theory," *Journal of Physical Chemistry Letters* 15 (2024): 2697–2707.

106. J. Cerdá, E. Ortí, D. Beljonne, and J. Aragó, "Optical Properties of H-Bonded Heterotriangulene Supramolecular Polymers: Charge-Transfer Excitations Matter," *Journal of Physical Chemistry Letters* 15 (2024): 7814–7821.

107. J. Cao, R. J. Cogdell, D. F. Coker, et al., "Quantum Biology Revisited," *Science Advances* 6 (2020): eaaz4888.

108. S. N. Mueller and B. T. Rouse, *Clinical Immunology*, 2nd ed., ed. R. R. Rich, T. A. Fleisher, W. T. Shearer, H. W. Schroeder, A. J. Frew, and C. M. Weyand (Elsevier Ltd., 2008), 421–431.

109. N. Sethuraman, S. S. Jeremiah, and A. Ryo, "Interpreting Diagnostic Tests for SARS-CoV-2," *JAMA* 323 (2020): 2249–2251.

110. C. A. Janeway, Jr., P. Travers, M. Walport, and M. J. Shlomchik, *Immunobiology: The Immune System in Health and Disease*, 5th ed. (Garland Science, 2001).

111. H. P. Roost, M. F. Bachmann, A. Haag, et al., "Early High-Affinity Neutralizing Anti-Viral IgG Responses Without Further Overall Improvements of Affinity," *Proceedings. National Academy of Sciences. United States of America* 92 (1995): 1257–1261.

112. M. F. Bachmann, U. Kalinke, A. Althage, et al., "The Role of Antibody Concentration and Avidity in Antiviral Protection," *Science* 276 (1997): 2024–2027.

113. G. Pantaleo, B. Correia, C. Fenwick, V. S. Joo, and L. Perez, "Antibodies to Combat Viral Infections: Development Strategies and Progress," *Nature Reviews Drug Discovery* 21 (2022): 676–696.

114. R. Kunert and D. Reinhart, "Advances in Recombinant Antibody Manufacturing," *Applied Microbiology and Biotechnology* 100 (2016): 3451–3461.